Performance of coded OFDM in very shallow water channels and snapping shrimp noise

Mandar Chitre
Acoustic Research Laboratory, National University of Singapore

S. H. Ong
Department of Electrical & Computer Engineering, National University of Singapore
Division of Bioengineering, National University of Singapore

John Potter
Acoustic Research Laboratory, National University of Singapore

***Abstract* – Although acoustic energy has been used effectively for point-to-point communications in deep-water channels, it has had limited success for horizontal transmissions in shallow water. Time-varying multipath propagation and non-Gaussian snapping shrimp noise are two of the major factors that limit acoustic communication performance in shallow water. Rapid time variation in the channel can limit the use of equalizers to compensate for frequency selective fading introduced due to multipath propagation. OFDM (orthogonal frequency division multiplexing), a communication technique widely used in wired and wireless systems, divides the available bandwidth across a number of smaller carriers, each of which experiences flat fading. This simplifies the equalizer structure and provides robustness against time-varying frequency-selective fading. Another source of signal degradation is impulsive noise from snapping shrimp, which affects several OFDM carriers at the same time. OFDM, when coupled with coding, can provide robustness against impulsive noise by distributing the energy for each bit over a longer period of time. We tested coded OFDM in a very shallow water channel in Singapore waters. The results show that it is a promising technique for use in very shallow, warm water channels.**

I. INTRODUCTION

Acoustic communications in shallow waters has been a challenging problem due to the unique channel characteristics of the underwater acoustic channel. Fading and multipath arrivals are believed to be the key issues in such channels [1][2]. Data rates of 20 kbps have been reported in Woods Hole harbour [2] while data rates of 15 kbps have been reported in the Baltic Sea [3]. The medium-range very shallow water channel, commonly found in coastal regions such as Singapore waters, is believed to be an extremely challenging channel. Many modems that have yielded good data rates in other shallow water channels have not been able to perform as well in Singapore waters. Based on channel measurements, it has been suggested that a high level of snapping shrimp dominated ambient noise and severe fading limit the performance of modems designed for operation in Gaussian noise [4].

In recent years, orthogonal frequency division multiplexing (OFDM) has been adopted in many communication systems [5]. OFDM divides the bandwidth into sub-carriers, each of which experiences frequency-flat fading. By introducing a cyclic prefix greater than the longest multipath delay, the equalizer becomes a single-tap filter for each sub-carrier. When coupled with channel coding, OFDM has the potential to achieve reliable communications in challenging channels. Several schemes based on coded OFDM have been suggested for the underwater channel [6][7]. However, we are not aware of any experimental results from the use of OFDM schemes in very shallow water channels and non-Gaussian noise.

In February 2005, we transmitted and recorded coded OFDM signals at various ranges in Singapore waters. Analysis of the signals received at a distance of 350 m in water depths of 15-20 m are presented in this paper.

II. COMMUNICATIONS SCHEME

The communication scheme used in this experiment was based on OFDM with a cyclic prefix. A differential phase shift keying (DPSK) modulation scheme with Gray coding was used to modulate each carrier. 2-DPSK, 4-DPSK and 8-DPSK were tested. Various serial concatenated convolution coding schemes were tested for their ability to reduce the bit error rate (BER) in the resulting communication link.

A. System Overview

Fig. 1 shows a simplified block diagram of the communication scheme. Source coding, decoding, A/D converter, D/A converter, anti-aliasing filters, power and pre-amplifiers have been omitted for simplicity. Enc 1 and Enc 2 represent convolutional encoders. Intrlv 1 and Intrlv 2 are random block interleavers. S/P and P/S blocks are serial to parallel conversion and parallel to serial conversion blocks respectively. The Mod and De-mod blocks perform

differential PSK modulation and detection, respectively. These blocks can be configured to rotate the phase of each modulated symbol according to a fixed table. This feature could be used for secure data communications, low peak-to-average power ratio transmissions or to modify the interpretation of the raw transmitted data in post-processing. IDFT and DFT are discrete inverse and forward Fourier transform blocks, commonly implemented using the fast Fourier transform (FFT) algorithm. The Cyclic Prefix block inserts the cyclic prefix, while the Symbol Sync block identifies the symbol boundaries and removes the cyclic prefix. The signal is modulated onto a carrier frequency (*Fc*) before transmission through the channel. The received signal is demodulated using the multiplier and low pass filter (LPF). Finally Viterbi Decode 1 and Viterbi Decode 2 are used for decoding the convolutional coded data while De-Intrlv 1 and De-Intrlv 2 undo the effects of the corresponding interleavers.

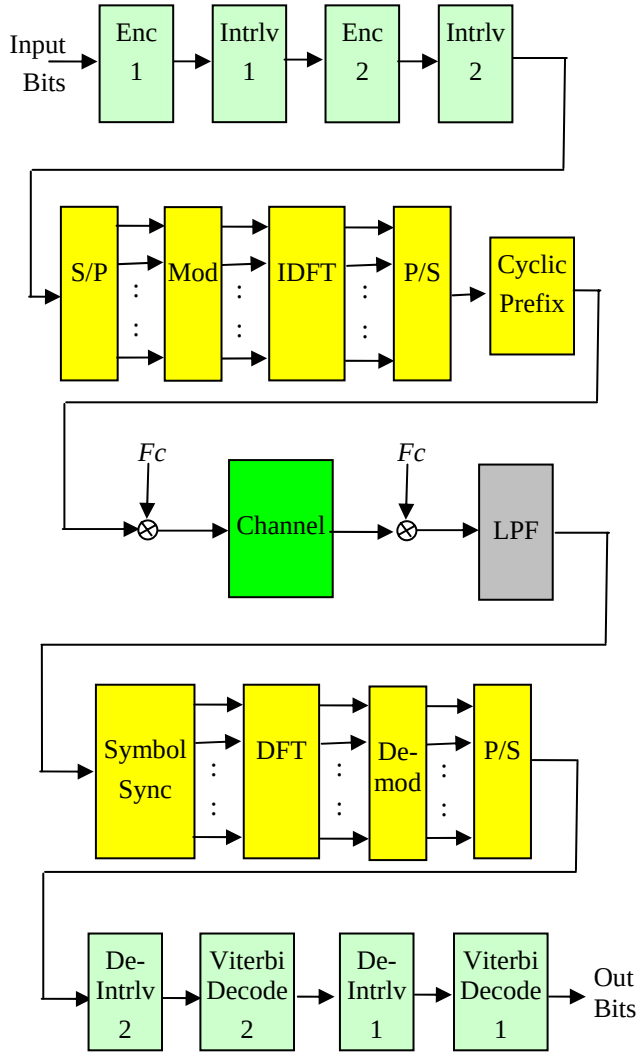

Fig. 1. Simplified system block diagram showing transmitter, channel and receiver

B. OFDM DPSK Modulation

Let N be the number of carriers used, f be the spacing between carriers, M be the length of the cyclic prefix and T be the length of the data block. We shall denote the modulated symbols at the input of the IDFT by $X_{j,t}$ where j is the carrier index (0 to N-1) and t is the time index (0 to T1). Similarly, we shall denote the symbols at the output of the DFT by $Y_{j,t}$. As long as the length of the cyclic prefix is more than the channel length, the channel can be modelled as a single tap filter with additive noise.

$$Y_{j,t} = H_{j,t} X_{j,t} + N_{j,t} \quad \ldots (1)$$

The coefficients of the channel filter tap $H_{j,t}$ vary with frequency and time for a shallow water channel. The noise $N_{j,t}$ is zero-mean additive but non-Gaussian due to the presence of snapping shrimp noise [4]. However, both $H_{j,t}$ and $N_{j,t}$ are not independent. Due to the impulsive nature of snapping shrimp noise, $N_{j,t}$ tends to be strongly correlated for different values of j but not correlated for different values of t. If the coherence bandwidth of the channel is much larger than the carrier bandwidth (f), $H_{j,t}$ is strongly correlated for different values of j. However, for our setup, we expect f to be comparable to the coherence bandwidth of the channel and consequently $H_{j,t}$ to be only weakly correlated between adjacent carriers. The coherence time of the channel determines the correlation of $H_{j,t}$ for different values of t. As the coherence time of the channel is expected to be much longer than the symbol time ($1/f$), we expect $H_{j,t}$ to be highly correlated for small differences in t.

In OFDM systems, it is common to use adjacent carriers for differential modulation. However, we opted to perform the differential PSK modulation over adjacent time indices as we expect $H_{j,t}$ to be more strongly correlated over time than over carrier index. Let $W_{j,t}$ be the PSK modulated symbols to be transmitted. $X_{j,t}$ is obtained by differential encoding of $W_{j,t}$.

$$X_{j,t+1} = X_{j,t} W_{j,t} \quad \ldots (2)$$

The received data $Y_{j,t}$ is converted to modulated PSK symbols $Z_{j,t}$ via the reverse process.

$$Z_{j,t} = \frac{Y_{j,t+1}}{Y_{j,t}} \quad \ldots (3)$$

From (1), (2) and (3), we have,

$$Z_{j,t} = \frac{H_{j,t+1} X_{j,t+1} + N_{j,t+1}}{H_{j,t} X_{j,t} + N_{j,t}} \quad \ldots (4)$$

As ambient noise is zero-mean, $E[N_{j,t}] = 0$ where $E[\cdot]$ represents the expectation operator. As the channel coefficients are highly correlated over time, $E[H_{j,t+1}] = E[H_{j,t}]$. The data is uncorrelated with the channel coefficients and the noise. Hence,

$$E[Z_{j,t}] = \frac{E[H_{j,t+1}X_{j,t+1}] + E[N_{j,t+1}]}{E[H_{j,t}X_{j,t}] + E[N_{j,t}]} \quad \ldots (5)$$
$$= \frac{E[H_{j,t+1}]X_{j,t+1}}{E[H_{j,t}]X_{j,t}} = W_{j,t}$$

Thus is clear that channel equalization is not needed provided that the cyclic prefix is longer than the channel length and the channel coherence time is much longer than the symbol time.

C. Symbol Synchronization

Symbol synchronization was performed using a maximum-likelihood (ML) method based on redundancy available in the cyclic prefix [8]. To reduce the noise in symbol estimation, we coupled the method described in [8] with a low pass filter.

The symbol synchronizer block identified the starting location of each symbol, removed the cyclic prefix and generated a *N*-sample symbol block at its output. The individual samples are obtained from this symbol block via the DFT operation.

D. Serial Concatenated Coding

The serial concatenated code was composed of an inner convolution code, an interleaver and an outer convolution code. The interleaver served to break burst errors from the inner code.

Various combinations of codes were tested. The constraint length and generator polynomials for the codes are shown in Table 1. The interleaver used was a pseudo-random block interleaver (MATLAB function – *randintrlv*). A hard-decision Viterbi algorithm was used to decode the data (MATLAB function – *vitdec*).

Table 1. Generators for the constituent convolution codes

Code Rate	**Constraint Length**	**Polynomials (Octal)**
1 / 2	8	247, 371
1 / 3	7	133, 145, 175
1 / 4	9	225, 520, 152, 215
2 / 3	5 4	23, 35, 0 0, 5, 13

E. Interleaver

In addition to the interleaver described in section I (D), a second interleaver was included after the coding process. This interleaver ensured that the errors at the input of the decoder for the inner code would be uncorrelated. Without this interleaver, these errors would be correlated due to the correlation of the channel fading and impulsive noise as described in section I (B). The interleaver used was also a pseudo-random block interleaver (MATLAB function – *randintrlv*).

III. EXPERIMENTAL SETUP

The experiment was performed in Singapore waters with a water depth of 15-20 m and a sandy-muddy bottom. The sea was calm with mild winds but strong currents. The transmitter and receiver systems were deployed from two vessels as described below (see Fig. 2).

The transmission system was deployed from a vessel at anchor. The transmitter consisted of a ruggedized PC with a D/A converter card, power amplifier and a ITC1042 transducer. The transducer was deployed at a depth of approximately 8 m using a 10 kg weight.

The receiver system was deployed from another vessel at anchor, about 350 m away from the transmitting vessel. The receiver consisted of a laptop, an external firewire A/D converter, a pre-amplifier (with band-pass filter) and a TC4013 hydrophone. The hydrophone was deployed at a depth of approximately 5 m using a 10 kg weight. The received signals were recorded for post-processing and analysis.

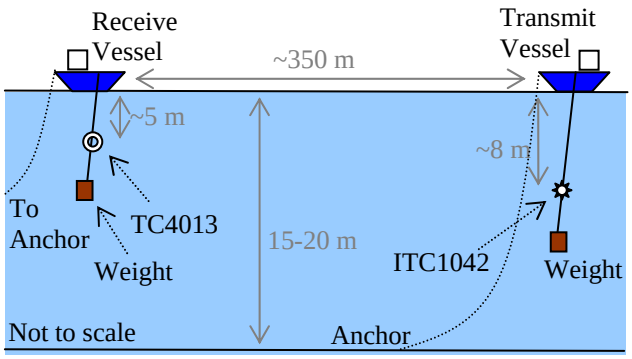

Fig. 2. Schematic representation of the experimental setup

The OFDM signal was generated with the following parameters:

$N = 64$

$M = 32$

$f = 375$ Hz

T = 2500

$Fc = 51$ kHz

The resulting signal has a bandwidth of 24 kHz centered at 51 kHz. Although the peak transmission performance of the ITC1042 is at about 80 kHz, it has an acceptable transmit performance in the signal band (39-63 kHz) which decreases with frequency. The total transmit source level was estimated to be approximately 170 dB re 1 μPa^2 @ 1m. The TC4013 has an almost flat sensitivity over the signal band.

The ambient noise at the location was analyzed and found to be non-Gaussian as expected. The average noise level was measured to be between 58-60 dB re 1 μPa^2/Hz. This amounts to a total ambient noise level of approximately 104 dB re 1 μPa^2 in the signal band. The amplitude probability distribution of the noise in the signal band was found to be

symmetric α-stable, as expected for snapping shrimp dominated ambient noise [4], with characteristic exponent 1.69 and scale parameter 6.8×10^4 μPa.

IV. RESULTS & DISCUSSION

The data collected during the experiment was analyzed via post-processing for performance under different modulation order and coding schemes. In addition, the data also provided valuable information about the channel. Both, channel measurements and communication performance results are presented in this section.

A. Channel Measurements

Fig. 3 shows the power spectral density (PSD) of the received signal compared to the ambient noise after passing through a band-pass filter to remove out-of-band noise. Although absorption is expected to increase with frequency, the received signal is stronger at higher frequencies. This is because the ITC1042 has stronger transmission efficiency at higher frequencies. At longer ranges, absorption will dominate and the trend will reverse. The local maxima and minima seen in the received signal are due to constructive and destructive interference in the two dominant arrivals (direct arrival and surface reflected arrival). The nulls are not as sharp as one would expect from a 2-ray model, as they are partially filled in by the weaker bottom reflected multi-path arrivals. The PSD only represents the average power over time. As the channel is time-varying, the nulls are also smeared out due to the variations in the channel response.

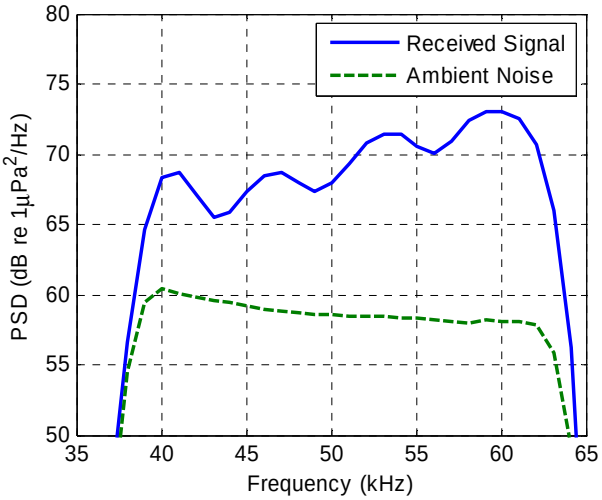

Fig. 3. Power spectral density of received signal (including noise) and ambient noise

Fig. 4 shows a spectrogram of the received signal. The time variation of the channel response can be clearly seen. The periodic variation in the channel may be due to the motion of the transducer and hydrophone induced by the surface waves. It may also be due to the movement of the sea surface and consequent change in arrival phase of the surface reflected component.

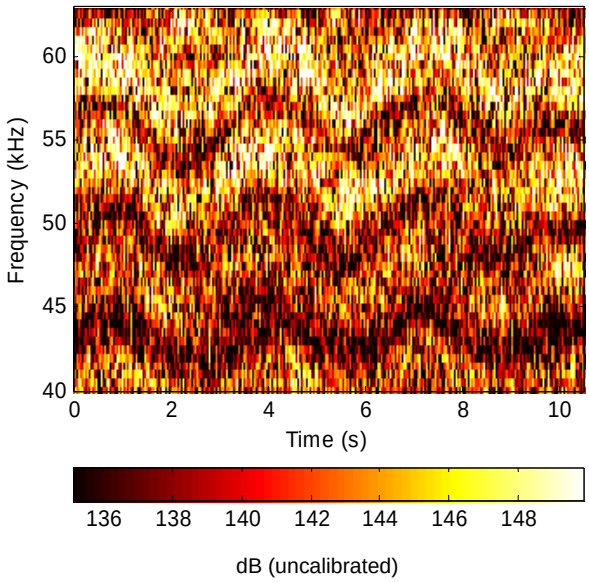

Fig. 4. Spectrogram of received signal showing time variation of the channel response

Fig. 5 shows the variation of the estimated channel impulse response over time. At 2.0 s and 6.0 s, two paths (direct arrival and surface reflected arrival) are can be clearly resolved. At 8.8 s, the surface reflected arrival is more diffuse and a new path is visible near sample 62. As the delay of this path is greater than the cyclic prefix, it is expected that the consequent inter-symbol-interference (ISI) will affect performance of the system. This was indeed observed in the analysis of the errors in DPSK detection performance without coding. Only a small fraction of the total transmitted data exhibit such a long a channel response.

B. Performance Measurements

The communication performance of the OFDM scheme was measured for different combinations of modulation order and coding schemes. All performance measurements in the following sections were made on a transmitted packet containing 160,000 coded symbols.

1) Performance without coding

With no error correction coding, the performance of the system in terms of BER was poor. As expected, the system showed an increase in BER with increased modulation order. The results are tabulated in Table 2.

2) Performance with coding without interleaving

With error correction coding, the BER performance of the system could be improved at the cost of reduced data rate. The performances of various combinations of modulation order and coding schemes are shown in Table 3. The rows where only code 1 rate is specified show results

from schemes which use convolution codes (see Table 1) for error correction. The rows with both code 1 rate and code 2 rate are specified show results from schemes with serial concatenated convolution codes for error correction. All schemes in this table disable interleaver 2 and enable interleaver 1 only during serial concatenated coding. None of the schemes tested met a BER criterion of $<10^{-4}$.

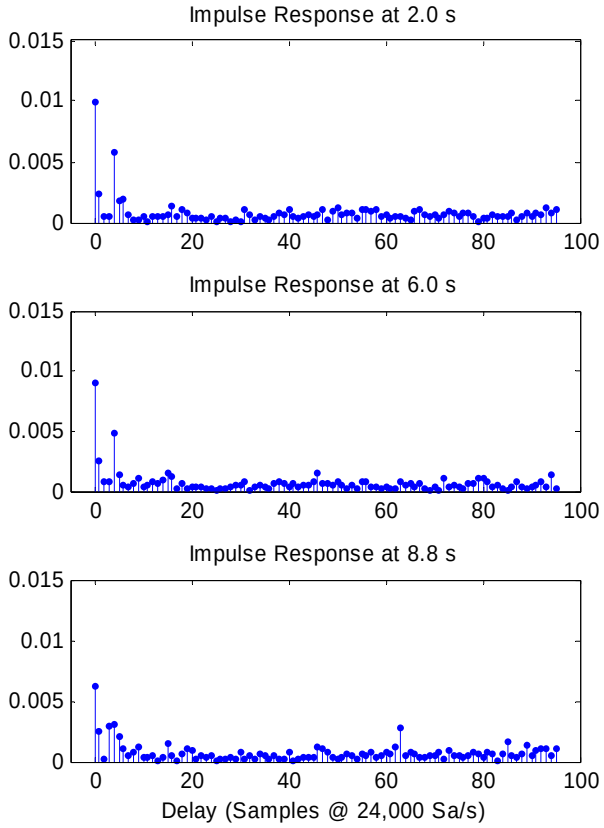

Fig. 5. Estimated impulse response at 3 time instants showing channel variation over time

3) Performance with coding and interleaving

The errors due to the ambient noise are correlated as snapping shrimp noise is impulsive and causes correlated errors on multiple carriers. Other errors introduced by the channel are often correlated due to slow fading. The performance of the communication system could be improved via interleaving without incurring any cost in terms of data rate but a small cost in transmitter and receiver complexity. The results from schemes with coding and interleaving are shown in Table 4. All schemes in this table use interleaver 2 while only the schemes with concatenated codes use interleaver 1. The results show that all schemes benefited from the use of the interleaver.

For a BER criterion of $<10^{-4}$, 4-DPSK with a serial concatenated code (outer code rate 1/2, inner code rate 1/3) seems to have the highest effective data rate of 5.3 kbps.

Table 2. Communication performance without coding

Modulation	Effective Data Rate (bps)	BER
2-DPSK	16,000	7.2×10^{-2}
4-DPSK	32,000	1.3×10^{-1}
8-DPSK	48,000	2.0×10^{-1}

Table 3. Communication performance with coding (with interleaver 2 disabled)

Modulation	Code 1 Rate	Code 2 Rate	Effective Data Rate (bps)	BER
2-DPSK	1 / 2	-	8,000	2.5×10^{-2}
2-DPSK	1 / 3	-	5,333	6.8×10^{-3}
2-DPSK	1 / 4	-	4,000	4.4×10^{-3}
4-DPSK	1 / 3	-	10,666	3.8×10^{-2}
4-DPSK	1 / 4	-	8,000	1.2×10^{-2}
4-DPSK	1 / 2	1 / 3	5,333	2.3×10^{-4}
8-DPSK	1 / 4	-	12,000	9.4×10^{-2}
8-DPSK	1 / 2	1 / 4	6,000	6.2×10^{-2}
8-DPSK	1 / 3	1 / 4	4,000	5.0×10^{-4}
8-DPSK	1 / 4	1 / 4	3,000	1.3×10^{-4}

Table 4. Communication performance with coding (with interleaver 2 enabled)

Modulation	Code 1 Rate	Code 2 Rate	Effective Data Rate (bps)	BER
2-DPSK	1 / 2	-	8,000	1.2×10^{-2}
2-DPSK	1 / 3	-	5,333	3.2×10^{-4}
2-DPSK	1 / 4	-	4,000	$< 10^{-4}$
4-DPSK	1 / 3	-	10,666	1.6×10^{-2}
4-DPSK	1 / 4	-	8,000	1.5×10^{-3}
4-DPSK	1 / 2	1 / 3	5,333	$< 10^{-4}$
8-DPSK	1 / 4	-	12,000	7.7×10^{-2}
8-DPSK	1 / 2	1 / 4	6,000	2.9×10^{-2}
8-DPSK	1 / 3	1 / 4	4,000	4.3×10^{-4}
8-DPSK	1 / 4	1 / 4	3,000	$< 10^{-4}$

V. CONCLUSIONS

In this paper, we have presented results from an experiment to test coded OFDM in a very shallow water channel with snapping shrimp dominated ambient noise. The experimental data suggests that the frequency response of the channel is time-varying. With the use of a cyclic prefix and DPSK modulation, OFDM can be successfully implemented on such a time-varying channel. However, the BER performance of uncoded OFDM is poor. With the use of serial concatenated convolution coding and an interleaver, the BER performance of OFDM can be improved significantly. However, the coding results in a reduced

effective data rate. We were able to demonstrate error-free transmissions at an effective data rate of up to 5.3 kbps during the experiment. This simple coded OFDM scheme performs well in a challenging underwater channel and may be used as a basis for further research in underwater acoustic communications.

VI. FURTHER RESEARCH

The performance of the communication scheme may be further improved via the use of more powerful coding schemes. The use of turbo coded OFDM with a channel-aware decoding scheme is currently being investigated. Although the long cyclic prefix and DPSK modulation simplify the receiver structure, they incur a cost in terms of system performance. To avoid this performance degradation, we are investigating channel estimation and equalization methods to allow use of coherent PSK and to reduce or eliminate the cyclic prefix.

ACKNOWLEDGMENTS

The sponsorship of the Defence Science and Technology Agency (DSTA), Singapore for this research is gratefully acknowledged. The authors would also like to express their appreciation for the help from Shiraz Shahabudeen, who helped with the data collection.

REFERENCES

[1] Catipovic, Josko A., "Performance limitations in underwater acoustic telemetry," IEEE J. Oceanic Eng. 15(3), pp.205-216, June 1990.

[2] Stojanovic, Milica, "Recent advances in high-speed underwater acoustic communications," IEEE J. Oceanic Eng. 21(2), pp.125-136, April 1996.

[3] Kebkal, Konstantin G., Rudolf Bannasch, Alexey G. Kebkal and Sergey G. Yakovlev, "Ultrasonic link for improved incoherent data transmission in horizontal shallow water channels," in Proc. OCEANS 2003, USA, pp.1786-1792, September 2003.

[4] Chitre M. A., John Potter & Ong Sim Heng, “Underwater acoustic channel characterisation for medium-range shallow water communications,” in Proc. OCEANS 2004, Japan, vol.1, pp.40-45, November 2004.

[5] Bingham J., “Multicarrier modulation for data transmission: An idea whose time has come,” IEEE Communications Magazine, 28, pp. 14-15, 1990.

[6] Lam W. K. & R. F. Ormondroyd, “A broadband UWA communication system: based on COFDM modulation,” in Proc. OCEANS '97, vol.2, pp. 862-869, 1997.

[7] Lam W. K. & R. F. Ormondroyd, “A novel broadband COFDM modulation scheme for robust communication over the underwater acoustic channel,” in Military Communications Conference (MILCOM 98), vol. 1, pp. 128-133, 1998.

[8] Van de Beek, J. J., M. Sandell & P. O. Borjesson, “ML estimation of time and frequency offset in OFDM systems,” IEEE Tr. Sig. Proc., 45 (7), pp. 1800-1805, 1997.